UCRL- 92243
PREPRINT

Approximate Treatment of Density Gradients in Rayleigh-Taylor Instabilities

Karnig O. Mikaelian

This paper was prepared for submittal
to Physical Review A

February 25, 1985

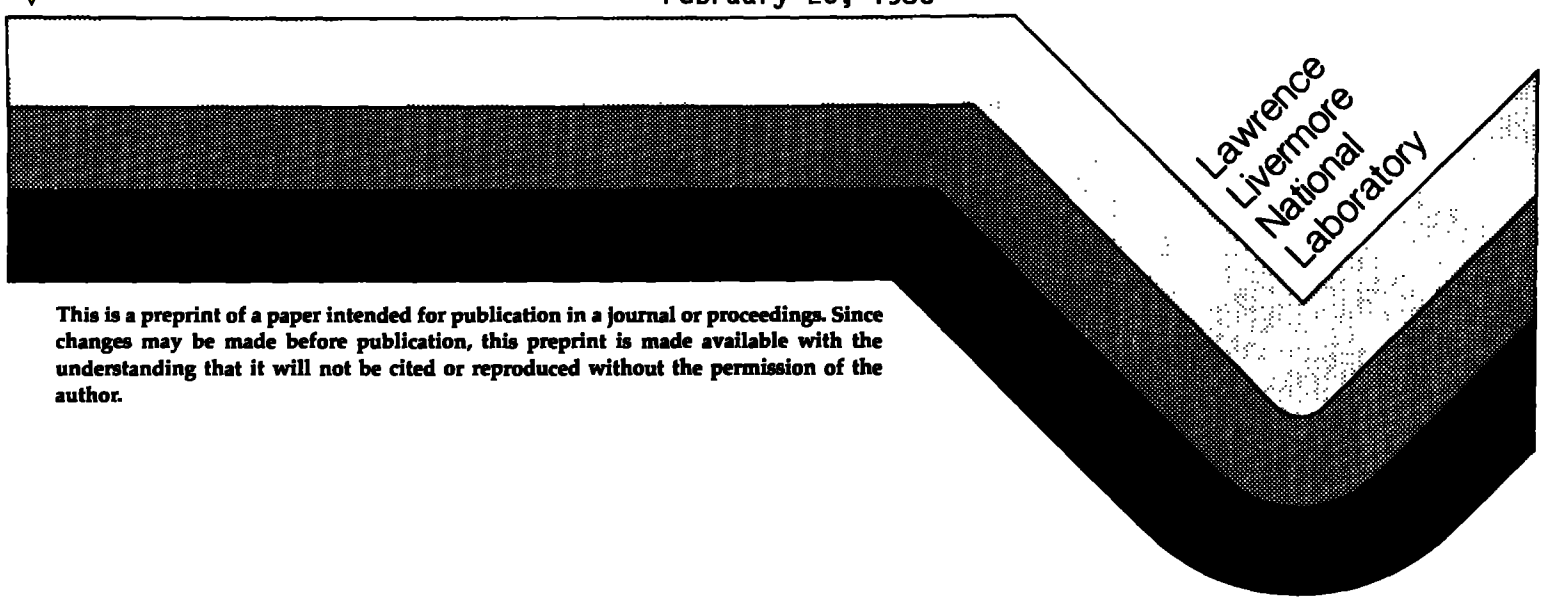

APPROXIMATE TREATMENT OF DENSITY GRADIENTS IN RAYLEIGH-TAYLOR INSTABILITIES*

Karnig O. Mikaelian

Lawrence Livermore National Laboratory

University of California

Livermore, California 94550

Abstract

We present an approximate method, based on a moment equation to derive explicit analytic formulas for the growth rate of Rayleigh-Taylor instabilities in fluids with density gradients. We illustrate with several examples and compare the results with our earlier method of treating a continuous density profile as a large number of fluid layers. The emphasis is on obtaining simple analytic formulas for the largest growth rate.

*Work performed under the auspices of the U.S. Department of Energy by the Lawrence Livermore National Laboratory under Contract No. W-7405-ENG-48.

I. INTRODUCTION

The Rayleigh-Taylor (RT) instability[1,2] occurs at the interface of two fluids subjected to an acceleration directed from the lower to the higher density fluid. The classical case refers to the density profile

$$\rho(y) = \begin{cases} \rho_1 & y < 0 \\ \rho_2 & y > 0 \end{cases} \tag{1}$$

with $\rho_1 < \rho_2$, and a constant acceleration $\vec{g}$ directed from ρ_1 to ρ_2. Perturbations at the interface $y = 0$ grow exponentially in time with the classical rate

$$\gamma_{classical} = \left[\frac{gk(\rho_2 - \rho_1)}{\rho_2 + \rho_1}\right]^{1/2} \tag{2}$$

where $k = 2\pi/\lambda$, λ = wavelength of perturbation.

Interest in the RT instability has been recently revived because of its important effect in Inertial Confinement Fusion[3,4] (ICF). Imperfections on the surface of a shell can grow large and cause the shell to break-up or to mix with the DT fuel. A number of calculations[4] and experiments[5] have shown that ablation tends to suppress the growth rate. Density gradients occur naturally in these calculations and experiments, and it is well-known[6] that density gradients also have the effect of reducing the growth rate of RT instabilities, particularly at short wavelengths. The fact that the shell has a finite thickness also tends to suppress the RT instability, in this case at longer wavelengths.

Earlier we presented[7] a method for calculating the growth rates in a system which consists of any number N of stratified fluids. While that method is adequate for the study of shells of finite thickness and arbitrary density

profiles, it does not yield simple closed-form expressions except in a few simple cases with $N \leq 5$. Continuous density profiles, in particular, are approximated by a large number N of fluid layers, and since the method invokes finding the eigenvalues of a (N-1) x (N-1) matrix, no analytic form can be written down.

Of course in most (practically all) cases there is no such analytic form. However, we found it useful to derive approximate analytic formulas based on a moment equation, and to check them against our earlier method. These formulas are useful as a simple and quick estimate of growth rates as functions of density profile and perturbation wavelength.

This investigation began when we discovered that the result presented in Ref. 6 differed from the result that one obtains using an equation derived by Chandrasekhar:[8] the two results agree in the long wavelength limit but disagree, by a factor of 2, in the short wavelength limit. We found that these were special cases of a more general equation that can be appropriately called a moment equation.

In the rest of this paper we present the general moment equation, apply it to several density profiles, and make some concluding remarks.

II. MOMENT EQUATION: DERIVATION AND DISCUSSION

Given a density profile $\rho(y)$ one finds the growth rate(s) γ by solving the second-order differential equation[8] ($D \equiv \frac{d}{dy}$)

$$D(\rho DW) + \frac{gk^2}{\gamma^2} WD\rho - k^2 \rho W = 0 \tag{3}$$

subject to appropriate boundary conditions. $W(y)$ is an eigenfunction associated with γ and, in general, there are infinitely many growth rates and associated eigenfunctions. In deriving Eq. (3) the assumptions of linearity, incompressibility, and the absence of viscosity, surface tension, and heat transfer are made (see Ref. 8).

Since Eq. (3) can be solved analytically for only a limited number of density profiles, we must use approximation techniques. Multiplying Eq. (3) by W^m and integrating over y we obtain

$$\frac{\gamma^2}{gk^2} = \frac{\int W^{m+1} D\rho dy}{k^2 \int \rho W^{m+1} dy + m \int W^{m-1} \rho (DW)^2 dy} \quad . \tag{4}$$

The integration is over $-\infty \leq y \leq \infty$ and we have thrown away "surface terms" $\rho W^m DW$ evaluated at $y = \pm\infty$. The exponent m is taken to be a non-negative number, but not necessarily an integer. We refer to Eq. (4) as the moment equation.

Eq. (4) reduces to

$$\frac{\gamma^2}{g} = \frac{\int WD\rho dy}{\int W\rho dy} \tag{5}$$

for $m = 0$ and

$$\frac{\gamma^2}{gk^2} = \frac{\int W^2 D\rho dy}{k^2 \int \rho W^2 dy + \int \rho (DW)^2 dy} \tag{6}$$

for $m = 1$.

Eq. (5) shows that there is an upper bound to the growth rate in the general class of continuous density profiles with no free surfaces:

$$\frac{\gamma^2}{g} \leq \frac{(D\rho)_{max}}{\rho_{min}} \tag{7}$$

where $(D\rho)_{max}$ is the max slope of the profile (finite because ρ is continuous) and ρ_{min} is the minimum density (non-zero because there are no free surfaces). Eq. (7) is significant because it is independent of k and it shows that the growth rate in such density profiles remains finite even in the limit of very short wavelength: compare Eq. (7) with Eq. (2) where $\gamma \to \infty$ as $k = 2\pi/\lambda \to \infty$.

Clearly Eq. (4) will yield the same γ for any m as long as the exact W is used. When an approximate W is used then γ depends on m, which we indicate by $\gamma_{[m]}$.

In the rest of this paper we choose $W_{classical}$ as our approximate eigenfunction W in all cases:

$$W_{classical} = e^{-k|y-y^*|} \tag{8}$$

where y^* denotes the location of the peak of the eigenfunction ($y^* = 0$ for the profile of Eq. (1)). An important consideration was its simplicity, since we shall integrate over it. Second, it has the proper behaviour if $\rho(y) \to$ constant as $y \to \pm\infty$. As we will see in our applications, the relatively simple expressions that we derive using Eq. (8) agree quite well with the numerical results where a large number N is used to simulate each particular density profile.

It is straightforward to show that $W_{classical}$ cannot be an exact eigenfunction for continuous density profiles, and hence the answer will

depend on m. We can, however, derive a simple relation between $\gamma_{[o]}$ and $\gamma_{[m]}$ valid for <u>all</u> density profiles. Since $W_{classical}$ satisfies $W^m(k) = W(mk)$ and $(DW)^2 = k^2W^2$, it follows that

$$\gamma^2_{[m]}(k) = \frac{1}{m+1}\,\gamma^2_{[o]}((m+1)k) \quad , \tag{9}$$

so we need to calculate only $\gamma_{[o]}$.

If we were to insist that γ be an exact expression for some density profile and hence be independent of m, Eq. (9) shows that this is possible only if $\gamma^2 = kF(\rho)$ where F is an arbitrary functional of ρ independent of k. Indeed, the classical γ has exactly this form, which is not surprising since Eq. (8) is the exact eigenfunction for that density profile. The form $\gamma^2 = kF(\rho)$, however, violates Eq. (7) which sets an upper bound for the growth rate independent of k. This contradiction is only a reflection of the fact that $W_{classical}$ is <u>not</u> an exact eigenfunction for continuous density profiles, and we will indeed find that γ depends on m, and the bound Eq. (7) is obeyed (when there are no free surfaces).

We found that the moment equation with m = 0, Eq. (5), gave a better answer than the higher m equations, particularly at short wavelengths. This is perhaps due to the presence of the $(DW)^2$ term in the general moment equation. That term is absent only for m = 0. We know that the slope $DW_{classical}$ cannot be correct because it is not continuous: $W_{classical}$ has a cusp at $y = y^*$ while W_{exact} <u>and</u> DW_{exact} must be continuous if the density profile $\rho(y)$ is continuous.[7]

We now turn to applications.

III. APPLICATIONS

A. Constant + Exponential Density Profile

Our first application is the density profile considered in Ref. 6:

$$\rho(y) = \begin{cases} \rho_1 + \frac{1}{2}\delta\rho e^{\beta y} & y \leq 0 \\ \rho_2 - \frac{1}{2}\delta\rho e^{-\beta y} & y \geq 0 \end{cases} \tag{10}$$

where $\delta\rho = \rho_2 - \rho_1$. Unlike the purely exponential density profile, this one cannot be solved analytically. Before using $W_{classical}$ to estimate the growth rate, we used our earlier method with N = 52 to simulate the above density profile and calculate the "exact" eigenfunctions and eigenvalues associated with the largest growth rates. Fig. 1 shows these eigenfunctions for k = 4, 8, 16. The density profile is also shown in Fig. 1: we have set $\rho_1 = 1$, $\rho_2 = 20$, and $\beta = 4$.

We see that all the eigenfunctions peak in the $y < 0$ region and get more localized as k increases. To obtain a simple analytic expression, however, we shall use $W_{classical}$ always peaking at y = 0, i.e., Eq. (8) with $y^* = 0$. For m = 0 we find

$$\frac{\gamma^2_{[0]}}{g} = \frac{k\beta}{k + \beta}\left(\frac{\rho_2 - \rho_1}{\rho_2 + \rho_1}\right) \tag{11}$$

which agrees with the expression derived in Ref. 6. Using Eq. (9) we find that the higher moment equations yield

$$\frac{\gamma^2_{[m]}}{g} = \frac{k\beta}{k(m + 1) + \beta}\left(\frac{\rho_2 - \rho_1}{\rho_2 + \rho_1}\right). \tag{12}$$

While in the limit $k \to 0$ both Eq. (11) and Eq. (12) reduce to the same classical expression in the limit $k \to \infty$

$$\frac{\gamma^2_{[o]}}{g} \to \beta\left(\frac{\rho_2 - \rho_1}{\rho_2 - \rho_1}\right) \tag{13}$$

while

$$\frac{\gamma^2_{[m]}}{\gamma^2_{[o]}} \to \frac{1}{m+1} . \tag{14}$$

The factor of 2 difference mentioned in our Introduction can be traced to using the moment equation with $m = 0$ or $m = 1$. The $m = 1$ equation can be found in Ref. 8 including surface tension and viscosity.

In Fig. 2 we compare the growth rates $\gamma/\sqrt{g}$ calculated in three different ways: our earlier method with $N = 52$, and the present method of using the moment equation with $m = 0$ and $m = 1$. Clearly $m = 0$ comes closer to the $N = 52$ result. The deviation at larger k which persists even for $m = 0$ is probably due to the fact that W_{exact} does not peak exactly at $y = 0$. However, considering the simplicity of Eq. (11), its description of γ over such a fairly wide range of k is quite satisfactory. A similarly good agreement was obtained for the density ratio $\frac{\rho_2}{\rho_1} = 2$. As far as we know this is the first time that the accuracy of Eq. (11), first derived in Ref. 6 for this specific density profile, has been checked by a completely different method.

B. Linear Density Profile

For our next application we chose a linear density profile,

$$\rho(y) = \begin{cases} \rho_1 & y < -\frac{d}{2} \\ (\rho_1 + \rho_2)/2 + (\rho_2 - \rho_1)(y/d) & -\frac{d}{2} \le y \le \frac{d}{2} \\ \rho_2 & y \ge \frac{d}{2} \end{cases} \tag{15}$$

It is worth reporting that our first choice for the eigenfunction was $W_{classical}$ peaking at $y = y^* = 0$. However, this gave substantially wrong answers (too small growth rates) when the density contrast ρ_2/ρ_1 was large. The choice $y^* = -d/2$ resulted in the following expression for the growth rate

$$\frac{\gamma^2[o]}{gk} = \frac{1}{1 + \frac{2\rho_1 dk}{\rho_2 - \rho_1}\left(1 - e^{-kd}\right)^{-1}} \tag{16}$$

which gave very good agreement with our N = 52 simulation of a linear density profile with $\rho_1/\rho_2 = 1/20$. With hindsight the choice $y^* = -d/2$ is clearly preferred since this is the location where $D\rho/\rho$ is maximum. While for long wavelengths this choice does not matter (they all go the classical limit), for shorter wavelengths it is crucial. Indeed, the "exact" eigenfunctions obtained by our previous N = 52 method all peak at $y = -d/2$. This is shown in Fig. 3 where we plot the density profile and the eigenfunctions associated with the largest growth rates for k = 4, 8, and 16. The scale for length is set by d = 1.

In the limit $d \to 0$ or, alternatively, in the long wavelength limit Eq. (16) reduces to the classical result

$$\frac{\gamma^2_{[o]}}{gk} \xrightarrow[k\to 0]{} \frac{\rho_2 - \rho_1}{\rho_2 + \rho_1} \quad , \tag{17}$$

while in the short wavelength limit it reduces to

$$\frac{\gamma^2_{[o]}}{g} \xrightarrow[k\to\infty]{} \frac{\rho_2 - \rho_1}{2\rho_1 d} \tag{18}$$

which can be seen to coincide with $D\rho/\rho$ at $y = -d/2$. (Note that $D\rho$ is not continous at $y = -d/2$ and must be obtained by averaging over $D\rho(y = -d/2 - \varepsilon) = 0$ and $D\rho(y = -d/2 + \varepsilon) = (\rho_2 - \rho_1)/d$, hence the factor 1/2 in Eq. (18)).

It is interesting to point out that if $\rho_1 = 0$ Eq. (16) reduces to $\gamma^2 = gk$. This is in fact an exact result valid for all density profiles with a free surface (see Ref. 7). In other words our choice for W happens to coincide with the exact eigenfunction for that profile if $\rho_1 = 0$. Consequently this result is independent of m. This would not have been the case if $y^* = 0$.

If $\rho_1 \neq 0$ then the growth rates depend on m, and we can use Equation (9) again to relate the higher moments to m = 0. In Fig. 4 we show the growth rates calculated for m = 0, m = 1, and for our N = 52 simulation of a linear density profile with the ratio $\rho_1/\rho_2 = 1/20$. The agreement between the N = 52 method and Eq. (16) is striking.

Such large density contrasts are of interest in ICF targets. For cases where the density contrast is not so large, i.e., $\rho_1 \sim \rho_2$, Eq. (16) predicts growth rates that are somewhat too small: if $\rho_1 = 1/2\ \rho_2$ then $\gamma_{[o]}$ is about 20% smaller than what the N = 52 method predicts at short wavelengths, $\lambda \lesssim d/3$. There is no problem at long wavelengths. We

found that this discrepancy is due primarily to the shape of the eigenfunction rather than the location of its peak: $W_{N=52}$ still peaks close to $y = -d/2$ but is broader than the exponentially decreasing $W_{classical}$.

C. Finite Thickness Density Profile

Our last example illustrates a shell of thickness t with density gradient lengths d_1 and d_2 on either side, as shown in Fig. 5. Assuming that $W = W_{classical}$ and that it peaks at the location shown in Fig. 5, we find

$$\frac{\gamma^2_{[o]}}{gk} = \frac{1}{1 + 2\rho_1 d_1 d_2 k\left[(\rho_2 - \rho_1)(1 - e^{-kd_1})d_2 + (\rho_3 - \rho_2)(1 - e^{-kd_2})d_1 e^{-k(d_1+t)}\right]^{-1}} \tag{19}$$

As a check note that if $\rho_3 = \rho_2$ we get back to the previous example. Similarly if $t = \infty$ or $d_2 = \infty$. As in the previous example, setting $\rho_1 = 0$ gives $\gamma^2 = gk$. Since we know that this is an exact result in this case also, we expect and indeed find Eq. (19) to be a good approximation if the density contrast ρ_2/ρ_1 is large.

In the very long wavelength limit Eq. (19) reduces to

$$\frac{\gamma^2_{[o]}}{gk} \xrightarrow[k\to 0]{} \frac{\rho_3 - \rho_1}{\rho_3 + \rho_1} \tag{20}$$

and in the very short wavelength limit

$$\frac{\gamma^2_{[o]}}{g} \xrightarrow[k\to \infty]{} \frac{\rho_2 - \rho_1}{2\rho_1 d_1} \tag{21}$$

These results are consistent with the fact that long wavelength perturbations probe the density profile at larger distances while short wavelength

perturbations, being more localized, see only a limited region of the density profile, hence the similarity of Eqs. (18) and (21).

In Fig. 6 we plot the growth rates γ as functions of k for 4 different density profiles. These are obtained from our analytic formulas. Profile A is the classical profile. Profile B shows the effect of replacing the sudden density jump of A by a linear density gradient: A and B overlap at long wavelengths, while at short wavelengths B is considerably more stable than A. C shows the effect of the finite thickness or, alternatively, the presence of a free surface, $\rho = 0$, on the other side of a shell. Now at short wavelengths C and B are identical (the free surface is too far to make any difference), while at longer wavelengths the free surface makes its presence felt by suppressing the growth rate: $\gamma_C < \gamma_B$ for $k \lesssim 1$ (the gradient length $d_1 = 1$ is used for scale, and we have set $t_1 = 1$, $d_2 = 0$). Finally, profile D is the case where both $t = 0$ and $d_2 = 0$, and Fig. 6 shows that while at short wavelengths B, C, and D all have identical growth rates, at longer wavelengths D is even more stable. The reason is that by eliminating t we have brought the stable free surface even closer.

Several special cases can be obtained from Eq. (19). In particular for $d_1 = d_2 = 0$, it reduces to

$$\frac{\gamma^2[o]}{gk} \xrightarrow[\substack{d_1 \to 0 \\ d_2 \to 0}]{} \frac{1}{1 + 2\rho_1\left[\rho_2 - \rho_1 + (\rho_3 - \rho_2)e^{-kt}\right]^{-1}} \quad . \tag{22}$$

This is, in fact, the case N = 3: a layer of fluid of density ρ_2 and thickness t between two semi-infinite fluids of densities ρ_1 and ρ_3. An explicit expression for the exact growth rates (there are two) was given in

Ref. 7. Eq. (22) agrees with neither of them except for trivial cases like $\rho_1 = 0$ or $\rho_3 = \rho_2$. The reason is twofold: 1) in general the eigenfunctions do not peak at the ρ_1/ρ_2 interface but somewhere between this and the other interface, and 2) the eigenfunctions have both an exponentially decreasing as well as increasing part in the middle layer.

To highlight the difference between our simple analytic formulas and the exact results, we consider the case $\rho_1 = 1/2\ \rho_2$ and $\rho_3 = 0$. Fig. 7 shows 2 density profiles and 4 growth rates: A and B refer to the same density profile; the curve labelled N = 3 is the exact result while the curve labelled m = 0 is based on Eq. (22). The agreement is good at short wavelengths, but bad at long wavelengths. In fact, Eq. (22) becomes negative at $k \lesssim 0.6$ (the scale is set by t = 1). While there <u>is</u> a stable mode in the exact result given by $\gamma^2 = -gk$, there is also a second and dominant mode which never becomes negative.

Curves C and D in Fig. 7 refer to the second density profile where the $\rho = 1$ to $\rho = 2$ abrupt transition is replaced by a linear density gradient of length $d_1 = 1$. Curve C is the result of using N = 52 to simulate this density profile, while D is based on Eq. (19) with $\rho_1 = 1$, $\rho_2 = 2$, $\rho_3 = 0$, $d_1 = 1$, $t_1 = 1$, $d_2 = 0$. There is fair agreement, within 20%, at short wavelengths, while at longer wavelengths $\gamma^2_{[0]}$ again goes negative, suggesting that the effect of the stable interface between $\rho = 2$ and $\rho = 0$ is overestimated in these formulas.

We should point out that the small density contrast $\rho_2/\rho_1 = 2/1$ was chosen in Fig. 7 to highlight were Eq. (19) fails. Indeed, for the larger density contrast used in Fig. 6 we found that Eq. (19) agrees very closely with the N = 52 results at both long and short wavelengths.

IV. REMARKS AND CONCLUSIONS

We derived simple, explicit analytic formulas for the growth rate of the Rayleigh-Taylor instability in a number of density profiles, and compared the results with our earlier technique. We checked the N = 52 result by comparing them with N = 27 and N = 77.

In all cases we have focused on the largest growth rate. There are many growth rates: in the case of finite N, there are N - 1 growth rates, and in the case of continuous density profiles there are infinitely many growth rates. While all of them are needed to find out how perturbations grow at each interface and feed-through from one interface to another,[9] the largest growth rate, which dominates at late times, can be used to assess the impact of a particular density profile and/or compare it with another one.

From the examples considered here it appears that the choice of the classical eigenfunction peaking where $D\rho/\rho$ peaks is a good one, especially when used in the m = 0 moment equation. One may try other functions or search for the one that maximizes $\gamma_{[1]}$ (this procedure is equivalent to solving the original differential equation--see Ref. 8), but the expressions quickly become too complicated, espeically when one tries to take into account the fact that the location of the peak is a function of both density and wavelength, as in Fig. 1.

We end with a brief summary of the present experimental situation: experiments with lasers[5] show that growth rates are reduced by a factor of about 2 from their classical values. However, one cannot separate the effects of ablation and density gradients. In a more recent classical type experiment with 3 fluids, where the acceleration is provided by rockets, it was found[10]

that a middle transitional or anti-mix layer of density $\rho_2 = \sqrt{\rho_1 \rho_3}$ suppresses, to some extent, the mix of the two fluids on each side. The experiments were well into the non-linear regime and cannot be properly analyzed in terms of a simple linear theory, but they do suggest that density gradients can be a stabilizing factor in Rayleigh-Taylor instabilities.

This work was supported by the U.S. Department of Energy Contract No. W-7405-ENG-48.

REFERENCES

1. Lord Rayleigh, Scientific Papers (Dover, New York, 1900) Vol. 2.
2. G. I. Taylor, Proc. Roy. Soc. London, Ser. A201, 192 (1950).
3. J. H. Nuckolls, L. Wood, A. Thiessen and G. Zimmerman, Nature (London) 239, 139 (1972); S. E. Bodner, Phys. Rev. Letters 33, 761 (1974).
4. R. L. McCrory, L. Montierth, R. L. Morse and C. P. Verdon, Phys. Rev. Letters 46, 336 (1981); M. H. Emery, J. H. Gardner and J. P. Boris, ibid 48, 677 (1982); R. G. Evans, A. J. Bennett and G. J. Pert, ibid 49, 1639 (1982).
5. J. D. Kilkenny et al., J. Phys. D13, L123 (1980); R. R. Whitlock et al., Phys. Rev. Letters 52, 819 (1984); J. Grun et al., ibid 1352 (1984).
6. R. Lelevier, G. J. Lasher, and F. Bjorklund, University of California Report No. UCRL-4459, 1959 (unpublished).
7. K. O. Mikaelian, Phys. Rev. Letters 48, 1365 (1982) and Phys. Rev. A 26, 2140 (1982).
8. S. Chandrasekhar, Hydrodynamic and Hydromagnetic Stability (Oxford University Press, London, 1968).
9. K. O. Mikaelian, Phys. Rev. A 28, 1637 (1983).
10. K. D. Burrows, V. S. Smeeton and D. L. Youngs, AWRE Report No. O 22/84, 1984 (unpublished).

FIGURE CAPTIONS

Fig. 1. Constant + exponential density profile (dashed line) and the eigenfunctions associated with the largest growth rates for k = 4, 8, and 16, calculated with N = 52. The scale is set by $\beta = 4$.

Fig. 2. The growth rate as a function of wavenumber for the constant + exponential density profile. The curve labelled N = 52 is obtained by using 52 fluid layers to represents the density profile (see Fig. 1 for representative eigenfunctions). The curves labelled m = 0 and m = 1 are the results of the corresponding moment equations.

Fig. 3. Same as Fig. 1 for the linear density profile. The scale is set by d = 1.

Fig. 4. Same as Fig. 2 for the linear density profile.

Fig. 5. Finite thickness density profile with linear gradients between 3 constant densities (see Section III C).

Fig. 6. Growth rates as functions of wavenumber k for 4 different density profiles (see text).

Fig. 7. Growth rates as functions of wavenumber k for 2 different density profiles (see text).

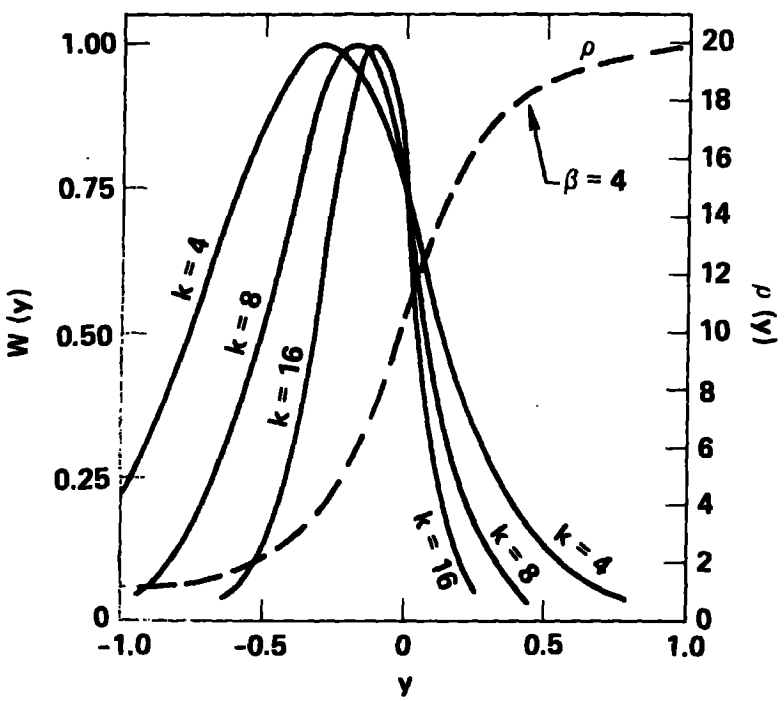
1.00
0.75
0.50
0.25
0
W (y)
-1.0
-0.5
0
0.5
1.0
y
20
18
16
14
12
10
8
6
4
2
0
ρ (y)
ρ
β = 4
k = 4
k = 8
k = 16
k = 16
k = 8
k = 4

Fig. 1

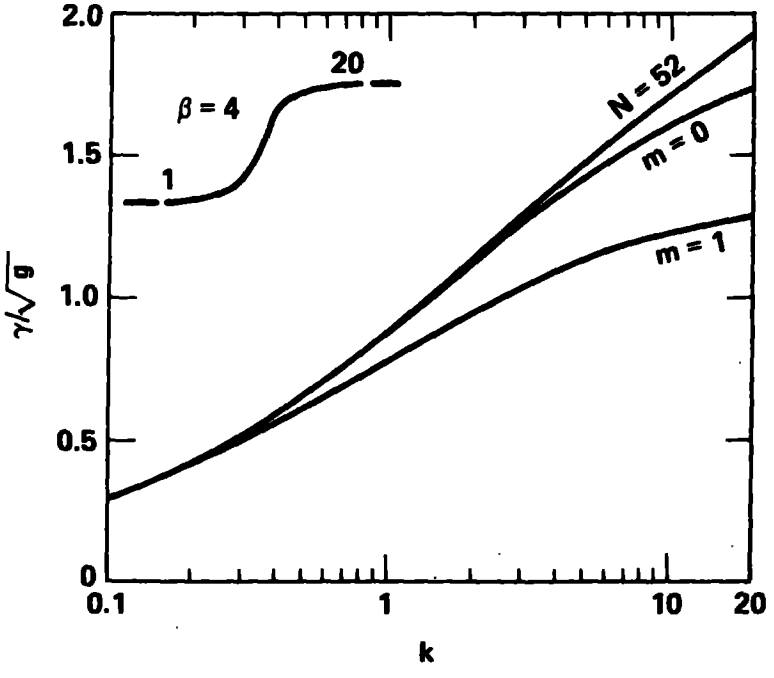

Fig. 2

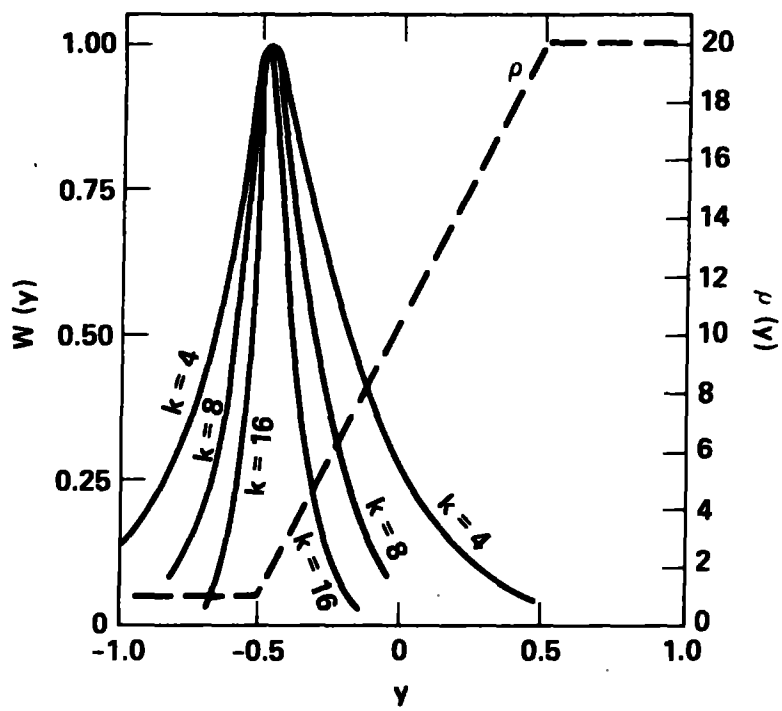
1.00
0.75
0.50
0.25
0
W (y)
-1.0
-0.5
0
0.5
1.0
y
20
18
16
14
12
10
8
6
4
2
0
ρ (y)
ρ
k = 4
k = 8
k = 16
k = 16
k = 8
k = 4

Fig. 3

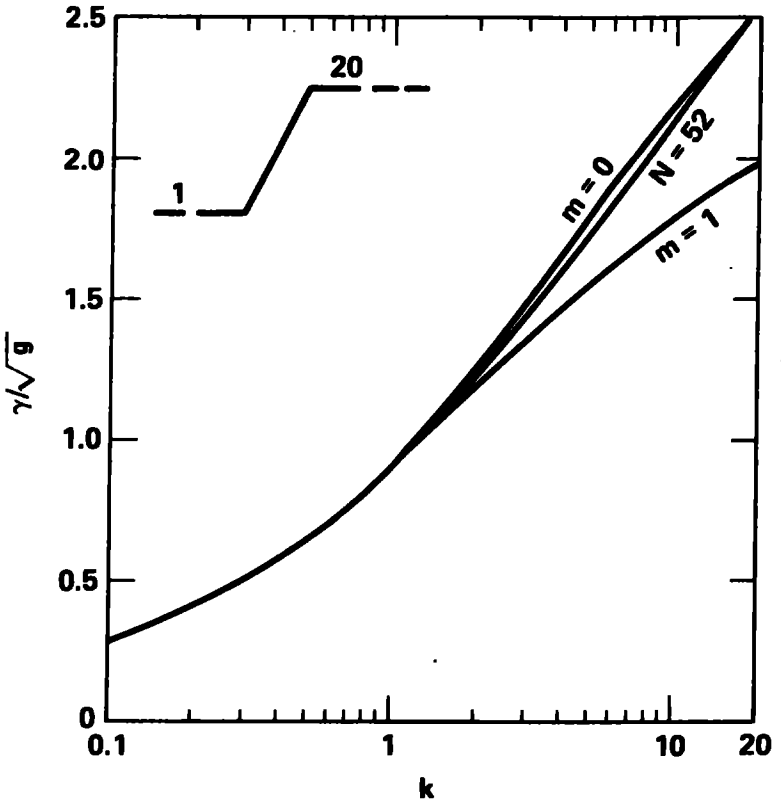

Fig. 4

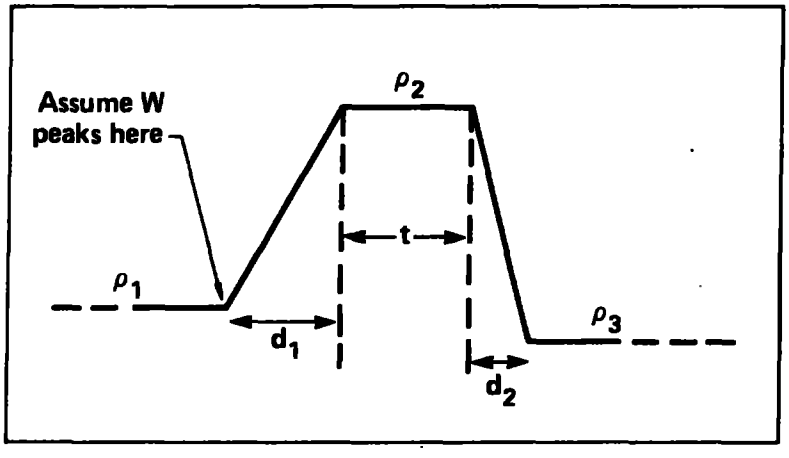

Fig. 5

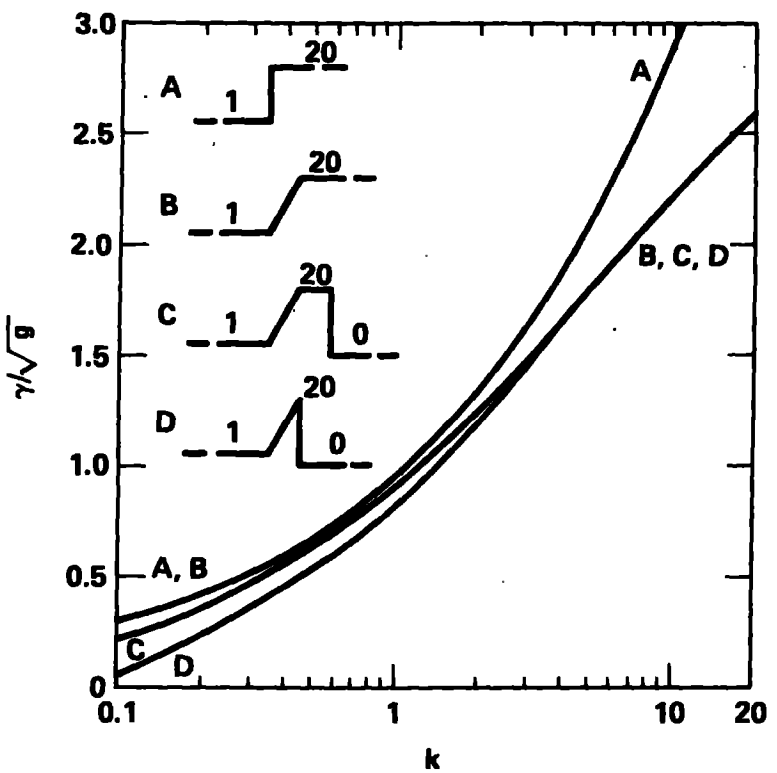

Fig. 6

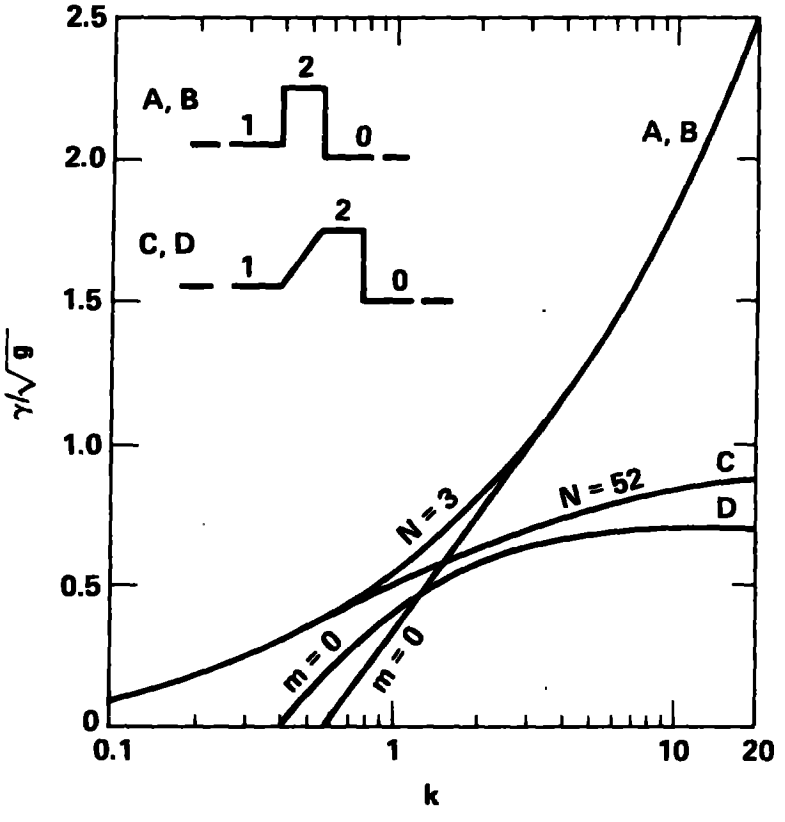
2.5
2.0
1.5
1.0
0.5
0
0.1
1
10
20
k
$\gamma/\sqrt{g}$
A, B
2
1
0
C, D
2
1
0
A, B
N = 3
N = 52
C
D
m = 0
m = 0

Fig. 7